The Dhaka University Journal of Earth and Environmental Sciences
https://www.banglajol.info/index.php/DUJEES

Flood Hazard Assessment of the Bangshi River Floodplain using an Integrated 1D/2D Coupled Hydraulic Model

Md. Jakir Hossain[1,2], A.S.M. Maksud Kamal[2], Md. Shakhawat Hossain[2], Md. Mostafizur Rahman[3] and Md. Zillur Rahman[2,*]

[1]*Groundwater Hydrology Division-2, Bangladesh Water Development Board, Dhaka 1205, Bangladesh*
[2]*Department of Disaster Science and Climate Resilience, University of Dhaka, Dhaka 1000, Bangladesh*
[3]*Department of Geology, University of Dhaka, Dhaka 1000, Bangladesh*

ARTICLE INFORMATION

Received : 28 November 2021
Accepted : 23 December 2021

Keywords:
Flood hazard assessment
Hydraulic model
Frequency distribution function
Pearson III distribution
Simulation

ABSTRACT

In the present study, the flood hazard of the Bangshi River, located in the Savar Industrial Area of Dhaka District, has been evaluated. The historical flood extent analysed from the Landsat satellite images suggests that most parts of the study area were flooded during the major flood events in Bangladesh. The flood flow data were fitted with different analytical frequency distribution functions, and it is found that the Pearson III distribution function best fits with the observed data based on the Chi-Squared statistical test. Then, the flood flow model of the Bangshi River as well as the surrounding floodplain area was developed using the HEC-RAS 1D-2D coupled hydraulic model. The model was simulated with an estimated flow of 100-year and 500-year return periods. The analysis of the historical flood data shows that the water level exceeds the danger level at the nearby monitoring station of the study area in different years. In the study area, devastating floods occurred in the years 1988 and 1998. The maximum flood level was 9.9 m during the flood event of 1988. The analysis of Landsat satellite images also shows that about 69% and 58% of the study area were flooded during the floods of 1988 and 1998, respectively. The roadways provide flood protection barriers in the western side of the study area for the flood water coming from the Bangshi River system unless the road is overtopped. The simulated result shows that about 68% and 79% of the study area will be inundated for the 100-year and 500-year return periods, respectively. The simulated maximum flood velocity for the 100-year and 500-year return period is 2.31 m/s and 4.52 m/s, and the flood duration for the same return periods is about 32.5 days and 48.95 days, respectively. The simulated flood depth, duration, and velocity maps can be used for any development activities within the study area.

Introduction

Flood is one of the most devastating natural disasters in the world caused by a combination of natural and anthropogenic processes (Rimi et al. 2019). Floods cause a considerable damage to social-economic aspects and affect the livelihoods of the people. The intensity and frequency of floods are increasing day by day in different regions of the world (Huq et al., 2020; Sampson et al., 2015). Due to climate change, extreme events (e.g., precipitation) are increasing in South Asia and causing severe flood events in recent years (Wax & Abdullah, 2007). In addition to climate change, land use change, deforestation, unplanned urbanization, upstream interventions are reducing the infiltration and increasing the runoff of the river basin (Huq et al., 2020). Flood events are being intensified by those changes in conjunction with climate extremities (Abedin et al., 2019). According to the climate projections by IPCC (Intergovernmental Panel on Climate Change), Bangladesh is one of the most vulnerable countries in the world due to an increase in monsoon precipitation and sea-level rise (Solomon et al. 2007).

Bangladesh is a deltaic country situated at the confluence of the world's three major rivers, namely, the Ganges, the Brahmaputra, and the Meghna. The unique geographic setting, hydrological and climate conditions, low-lying floodplain, and depression topography make this area extremely vulnerable to flood hazards. As the country is mostly floodplain (80 %), it is well-known as one of the most flood-prone countries in the world, where one fifth to one-third of the country is annually flooded due to overflowing rivers during the monsoon (June to

* Corresponding Author
E-mail: zillur@du.ac.bd (Md Zillur Rahman)

DOI: https://doi.org/10.3329/dujees.v10i3.59082

September). The synchronization of upstream riverine floods with the heavy rainfall within the land boundary of the country makes the flood situation worst for the whole nation. Every year, at least 20% of the areas of the country are inundated, and in severe cases, 68% of areas of the country are inundated (Huq et al., 2020). Floods cause widespread and multifarious damages to physical infrastructures, crops, and social disruptions affecting the livelihoods of millions of the people with direct and indirect economic losses. The country has experienced massive floods in 1974, 1984, 1987, 1988, 1998, 2000, 2004, and 2020 (Islam & Sado, 2000). The floods in 1988 and 1998 were the most severe in the past century, which inundated about 61% and 68 % of the total area of the country, respectively (Uddin and Matin 2021). Flood hazards are becoming increasingly frequent and acute in recent years due to human interventions and socio-economic development activities in the floodplain areas on an ever-increasing scale. The unplanned urbanization and continuous industrial development activities around the floodplain of the Bangshi River located in Savar and the adjoining area may trigger the flood event and increase the damage by increasing exposure in the flood-prone area. Therefore, it is especially important to delineate the flood-prone area in advance to take protective measures to minimize the flood damage.

Although structural flood protection measures are being practiced for a long time and contributing successfully for some places, they do not seem to be sufficient to effectively reduce the risk of flood. There are also some adverse effects of structural flood protection measures on river ecosystem and health (Mondal et al., 2021) Therefore, it is necessary to include the non-structural measures, especially flood prediction for preparedness and mitigate the flood risk. Hydraulic modelling analysis can perform flood simulation and can provide precise information in advance about areas that will be inundated. Hydraulic modelling can also perform one-dimensional (1D) and two-dimensional (2D) simulations of the flood wave propagation in the natural channel for different flood scenarios. The 1D modelling approach has some limitations for overflow analysis, though it is particularly useful for flood forecasting and warning. Once the water begins to overflow, it becomes a 2D phenomenon. Hence, this study considered a combined one dimensional (1D) and two dimensional (2D) hydrodynamic model for simulating the flood inundation in the studied area. In coupled 1D/2D model, the floodplain is considered as a 2D part, and the river channel is represented as a 1D part. Thus, the similar physical behaviour of flood wave propagation is represented with the coupled 1D/2D model. The Hydrologic Engineering Center River Analysis System (HEC-RAS) software can simulate 1D, 2D, and coupled 1D/2D models. Although few studies were conducted for different rivers in Bangladesh using 1D model (Mark et al., 2001; Masood & Takeuchi, 2011) and 1D/2D couple hydraulic model (Roy et al. n.d.) for flood hazard mapping, the coupled 1D/2D model approach can provide precise and reliable flood hazard mapping for preparing flood zoning maps. Thus, this study focused on flood hazard mapping using a coupled 1D/2D models in the newly urbanized and industrial areas of Savar and Dhamrai upazilas (sub-districts) in Bangladesh (Figure 1)) to reduce the flood risk.

Study Area

The study area is situated within Savar and Dhamrai upazilas of Dhaka District (Figure 1), almost in the central part of Bangladesh. Savar is located about 24 kilometres away from the northwest side of Dhaka city. It is well-known as an industrial zone beside the Dhaka metropolitan city. The study area is placed on the floodplain of the Bangshi River, a distributary of the Jamuna River. The area is covered by multiple abandoned channels, wetlands created from the depressions of floodplains, and a newly developed urban landscape. Most of the areas of the floodplains and depressions have been filled with sand and clay to raise the elevation for urban development. The Bangshi River, which was once the lifeline of the Savar town, has been polluted miserably due to dumping of the industrial waste into the river (Rahman et al., 2012). The detailed land use and land cover (LULC) map of the study area is shown in Figure 2. The detailed methodology of preparing land use and land cover map is described in Appendix (A1). The LULC map of the study area shows that the area is badly planned for urban development, which may hamper the natural flow path of the drainage system and produce severe flooding from the combination of both urban and riverine floods.

The topography of the study area is mostly flat. The Bangshi River formed this flat area by overbank deposition. Due to channel avulsion, the river shifted its course and created abandoned channels that represent the topographic depressions. The study area shows a slight slope toward the Bangshi River, which ultimately drains the area. The area is in a subtropical to tropical monsoon climatic zone, which experiences heavy precipitation. Based on the measurements from the nearby of rainfall measuring stations of BWDB, it is shown that the average annual rainfall in the wet season is about 2000 mm with maximum rainfall (about 90%) occurring between May to October. Most of the rainfall that falls within the study area is drained to the Bangshi river through the drainage network. The area is also situated on the lower eastern extremity of the Brahmaputra-Jamuna floodplain physiographic unit, which is also known as the young Brahmaputra floodplain (Hossain et al., 2017). The north-south elongated floodplain unit consists of recent (Holocene) alluvial deposits (Mourin et al., 2017, 2019).

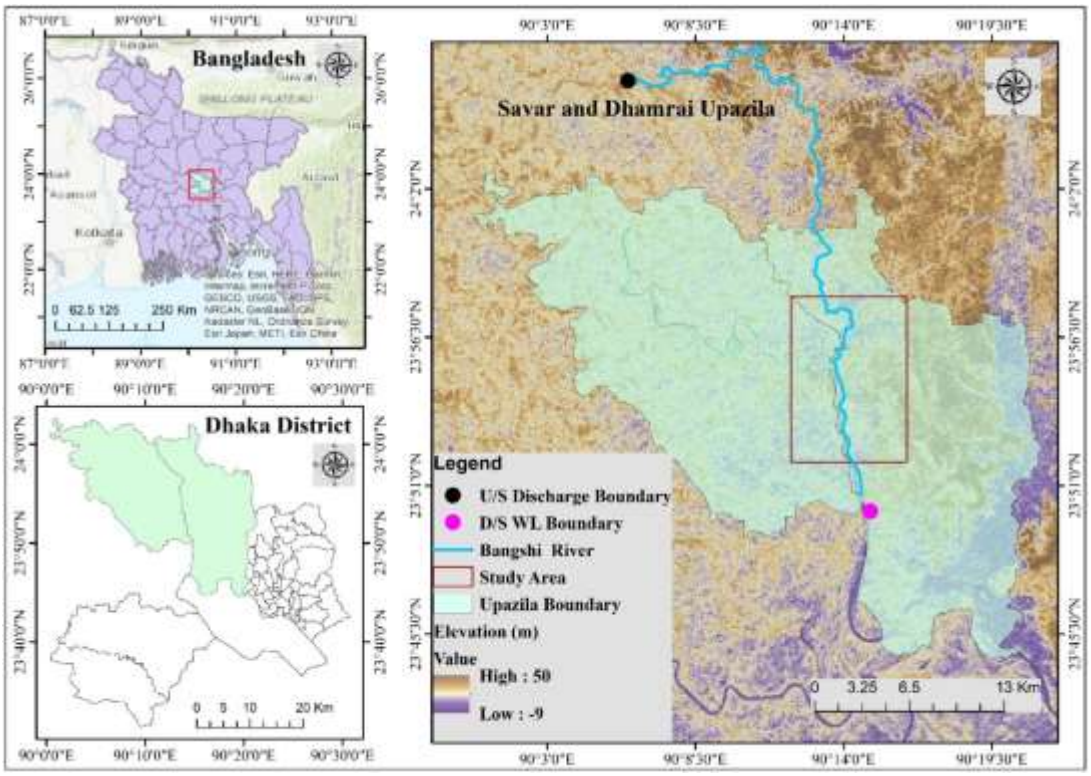

Figure 1: Location map of the study area. The map shows the focused study area in the rectangular box, the upstream (U/S) discharge boundary, the downstream (D/S) water level (WL) boundary, the river network, and the outline of the administrative boundary. In the background, the topographic elevation of the surrounding area is shown

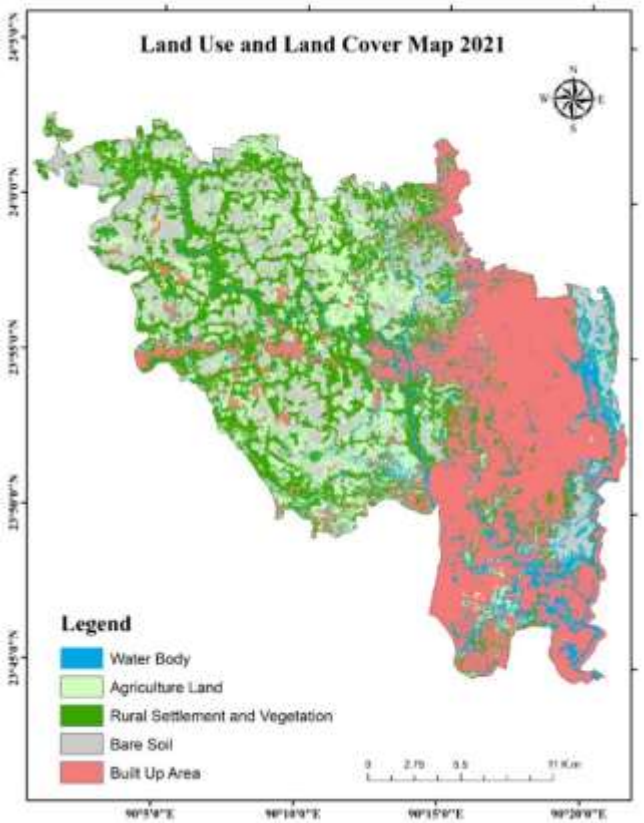

Figure 2: The land use and land cover (LULC) map of Savar and Dhamrai upazilas. The LULC map was prepared using Landsat 8 satellite images of January 2021

Materials and Methods

Flood Frequency Analysis

The flood frequency analysis was performed to estimate the river flow values corresponding to 100-year and 500-year return periods. Flood frequency analysis was conducted using the discharge and water level data (Karim and Chowdhury 2009; Roy et al. 2019). The bimonthly discharge data and 3-h water level data from 1980 to 2020 were collected from Bangladesh Water Development Board (BWDB). The water level and river cross-section data were in term of Public Work Datum (PWD), which is about 0.46 m below the mean sea level (FFWC). This study considered the annual maximum data series for the analysis. The long-term water level hydrograph and danger level for a monitoring station (SW14.5) of the Bangshi River located at Nayarhat, Savar is shown in Figure 3. The danger level of the monitoring station was collected from the Flood Forecasting and Warning Center (FFWC). Before conducting the frequency analysis, the data homogeneity and stationarity were checked (Grimaldi et al., 2011; Haan, 1977). The statistical frequency distribution predicts the future possibility or likelihood of the occurrence of a flood event in a particular location. Many probability distribution functions are available for frequency analysis of extreme events but there is no universally accepted model for frequency analysis (Haan 1977; Roy et al. 2019). In this study, frequency analysis was performed using five widely used probability density functions (PDF) in hydrology to find the best fitted model (Grimaldi et al., 2011; Haan, 1977) for our data. This study considered Pearson III, Gamma, Gumbel, Log Person III, and Log-Normal Distribution for frequency analysis. These distributions are mostly used for the frequency analysis of discharge and water level in Bangladesh (Karim and Chowdhury 2009; Roy et al. 2019).

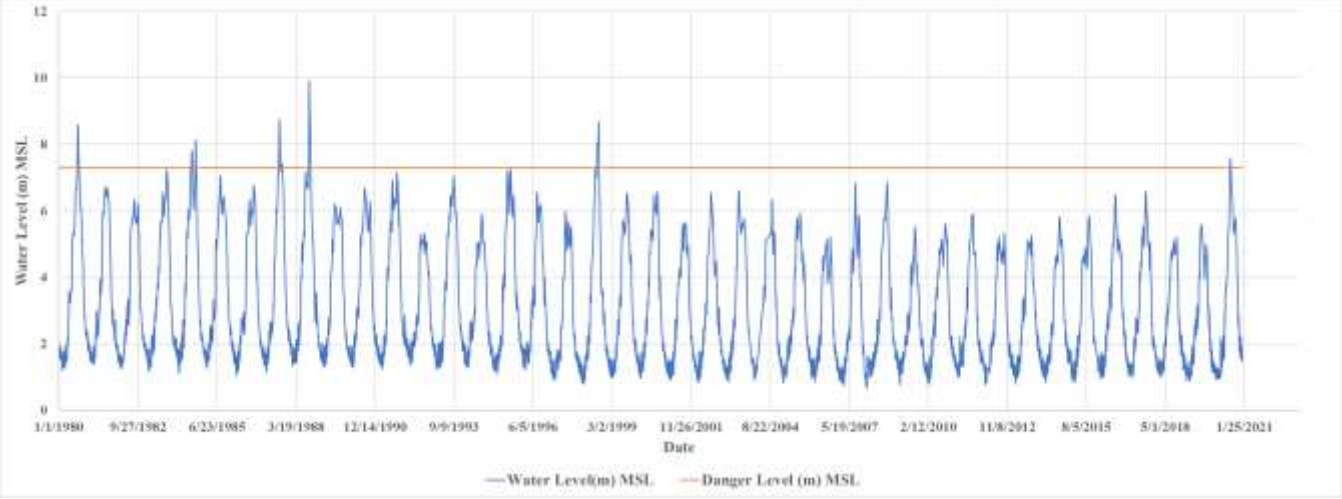

Figure 3: River water level hydrograph of the Bangshi River at Nayarhat station, Savar. The hydrograph shows that the water level exceeds the danger level causing severe flood at different years

The general equation of hydrologic frequency analysis was developed by Chow (1951), and the extreme value distribution introduced by Gumbel (1941) is widely used for hydrologic and meteorological studies. The general equation for Gumbel distribution with return period T is as follows:

$$X_T = \bar{X} + K\sigma_x \quad (1)$$

where X_T = value of X for return period T

$\bar{X}$ is the mean of the sample

σ_x is the standard deviation of the sample

K is the frequency factor, which is expressed as below:

$$K = \frac{Y_t - \bar{Y}_n}{S_n} \quad (2)$$

where Y_t is the reduced variate, which is computed using the following equation:

$$Y_t = -\left[ln.\, ln\left(\frac{T}{T-1}\right)\right] \quad (3)$$

The value $\bar{Y}_n$ and S_n are selected from the Gumbel's extreme value distribution table depending upon the sample size.

The probability density function (PDF) Pearson Type-III distribution is calculated using the following equation (Haan 1977):

$$f(x) = \frac{1}{\alpha\Gamma(\beta)}\left[\frac{x-\upsilon}{\alpha}\right]^{\beta-1} exp\left[-\frac{x-\upsilon}{\alpha}\right] \quad (4)$$

Where α, β and υ are the shape scale, and location parameters, respectively, to be estimated from the sample and $\Gamma(\beta)$ is the gamma function. The mathematical expression of the other probability density functions can be accessed in the standard literature (Grimaldi et al., 2011; Haan, 1977).

Goodness-of-fit test

The goodness-of-fit test was carried out to show how well the specific probability density function fits

the data. It measures the capability of the random sample to conform to a theoretical probability density function (Baidya et al., 2020; Hassan et al., 2019). The best fitted frequency distribution function is selected based on the goodness of the fit statistics. There are different methods for fitting a representative distribution. This study considered the Chi-Squared ($\chi 2$) test, which is commonly used in different studies (Baidya et al., 2020; Hassan et al., 2019) for checking the goodness-of-fit for the given data.

Chi-Squared ($\chi 2$) Test

The Chi-Squared test is a statistical hypothesis test. The test statistic is given by:

$$\chi^2 = \sum_{j=1}^{l} \frac{(O_j - E_j)^2}{E_j} \quad (5)$$

where, O_j= observed frequency; j = observations' number

Expected frequency $(E_j) = F(Y_2) - F(Y_1)$

where, F = cumulative distribution function

$l = 1 + log_2 m$

where, m = sample size.

The flood frequency analysis was conducted using the U.S. Army Corps of Engineers Hydrologic Engineering Center's (HEC) Statistical Software Package (HEC-SSP) (Harris et al., 2008). This software permits users to execute statistical analyses of hydrologic data. By using the software, the discharge and water level values for 100-year and 500-year return periods were estimated using the best-fitted frequency distribution function.

Remote Sensing Based Historical Flood Mapping

The extent of the historical flood within the study area was assessed using remote sensing satellite images collected from the USGS Landsat (Path = 137 and Row = 04) archive database. The image acquisition dates (1988-09-14 and 1998-09-26) were selected based on the maximum flood water level hydrograph for the floods of 1988 and 1998. As the Landsat satellite uses an optical sensor and it could not penetrate the atmospheric cloud, we tried to collect the cloud-free images very near to the maximum water level. Therefore, there is more than a one-week difference between the image acquisition date and the maximum water level (the maximum water level was 9.9 m on September 03 and 8.63 m during image acquisition time for the flood of 1988, On the other hand, the maximum water level was 8.68 m on the 11th of September, but the image was taken when the water level was 7.44 m for the flood of 1998) that occurred at the nearby station. As a result, the estimated inundation extent could be considerably underestimated. The water body was delineated using the Normalized Difference Water Index (NDWI). The NDWI is derived from the Near-Infrared (NIR) and Green (G) bands of the Landsat 5 TM images using the following formula (Gao 1996):

$$NDWI = \frac{(G - NIR)}{G + NIR} \quad (6)$$

The range of the index value is -1 to +1. A value greater than zero indicates a water body, which is represented as the flooded area and other values (less than or equal to zero) are represented as the non-flooded area. Although there are a lot of techniques for estimating flood extent, this formula has greater accuracy in delineating flood extent (Jain et al., 2005; McFeeters, 1996). This is why, this formula is used to delineate the flood extent.

Hydraulic Model

The hydraulic model of the studied area was created using the Hydrologic Engineering Center's River Analysis System (HEC-RAS) software. This software could be used for one-dimensional steady flow, one- and two-dimensional unsteady flow calculations, coupled 1D/2D flow, sediment transport/mobile bed computations, and water temperature/water quality modelling. This study considered a coupled 1D/2D model for simulating the flood inundation of different return periods. As the study area is a low-lying floodplain area of the Bangshi River system, the 1D hydraulic model cannot perform well for its complex urban development, flow reversal, and low hydraulic gradient. The model was developed defining the 1D model toward the river channel and the 2D model for the floodplain area. HEC-RAS solves fully two-dimensional (2D) Saint-Venant equations:

$$\frac{\partial h}{\partial t} + \frac{\partial (hu)}{\partial x} + \frac{\partial (hv)}{\partial y} = q \quad (7)$$

$$\frac{\partial u}{\partial t} + u\frac{\partial u}{\partial x} + v\frac{\partial u}{\partial y} - f_c v = -g\frac{\partial z_s}{\partial x} + \frac{1}{h}\frac{\partial}{\partial x}\left(v_{t,xx}\, h\, \frac{\partial u}{\partial x}\right) + \frac{1}{h}\frac{\partial}{\partial y}\left(v_{t,yy}\, h\, \frac{\partial u}{\partial y}\right) - \frac{\tau_{b,x}}{\rho R} + \frac{\tau_{s,x}}{\rho h} \quad (8)$$

$$\frac{\partial v}{\partial t} + u\frac{\partial v}{\partial x} + v\frac{\partial v}{\partial y} + f_c u = -g\frac{\partial z_s}{\partial y} + \frac{1}{h}\frac{\partial}{\partial x}\left(v_{t,xx}\, h\, \frac{\partial v}{\partial x}\right) + \frac{1}{h}\frac{\partial}{\partial y}\left(v_{t,yy}\, h\, \frac{\partial v}{\partial y}\right) - \frac{\tau_{b,y}}{\rho R} + \frac{\tau_{s,y}}{\rho h} \quad (9)$$

where, h represents the depth of water (m); u and v represent the velocity in the x and y directions (m s^{-1}); q represents the source/sink flux term; z_s represents the elevation of the surface (m); g denotes the acceleration due to gravity (m s^{-2}); ρ represents the water density (kg m^{-3}); τ_{bx}, and τ_{by} denotes the bottom shear stress on x and y directions and $\tau_{s,x}$ and $\tau_{s,y}$ denotes surface wind stress directions; R is the hydraulic radius and f_c represents the Coriolis (s^{-1}) force.

For developing the hydraulic model, the necessary data was collected from different relevant organizations. The topographic elevation (Figure 1) of the catchment was collected from 30 m resolution SRTM digital elevation model data from the NASA website (https://dwtkns.com/srtm30m/). The Digital Elevation

Model (DEM) data prepared from the topographic survey of the study area was also merged with the SRTM data and used as a terrain in the model. The data pre-processing was performed using ArcGIS 10.8 software. The pre-processed topographic data was used in HEC-RAS for developing the hydraulic model. For developing the 1D hydraulic model, the river cross-section data is given as the input parameter data to define the geometry of the channel. The river cross-section, surface water level, and river discharge data of the Bangshi and Dhaleswari rivers were collected from the BWDB. The cross-section of the river at the key points is shown in Appendix (A5.1 to A5.4). The flood hydraulic model was extended up to nearby gage stations to assign suitable boundary conditions at the monitoring station (Figure 1). The upstream boundary of the model was assigned using discharge data and the downstream boundary was assigned using water level data. The model was calibrated and validated using mean daily water level data at the Nayarhat location (SW14.5). The water level dataset for 2020 was used for model calibration and the validation was performed using the dataset for 2019. Several trial simulations were performed using a variable Manning's roughness coefficient ranging from 0.010 to 0.025. The simulation results show that the surface elevation get increased by the higher value of the Manning coefficient, which is consistent with the law of water flowing. Finally, the Manning's roughness value of 0.17 for different cross-sections of the channel was found to produce an acceptable result of simulated water level compared with observed water level. The calibration and validation of hydrograph are shown in Figure 4 (a) and Figure 4 (b).

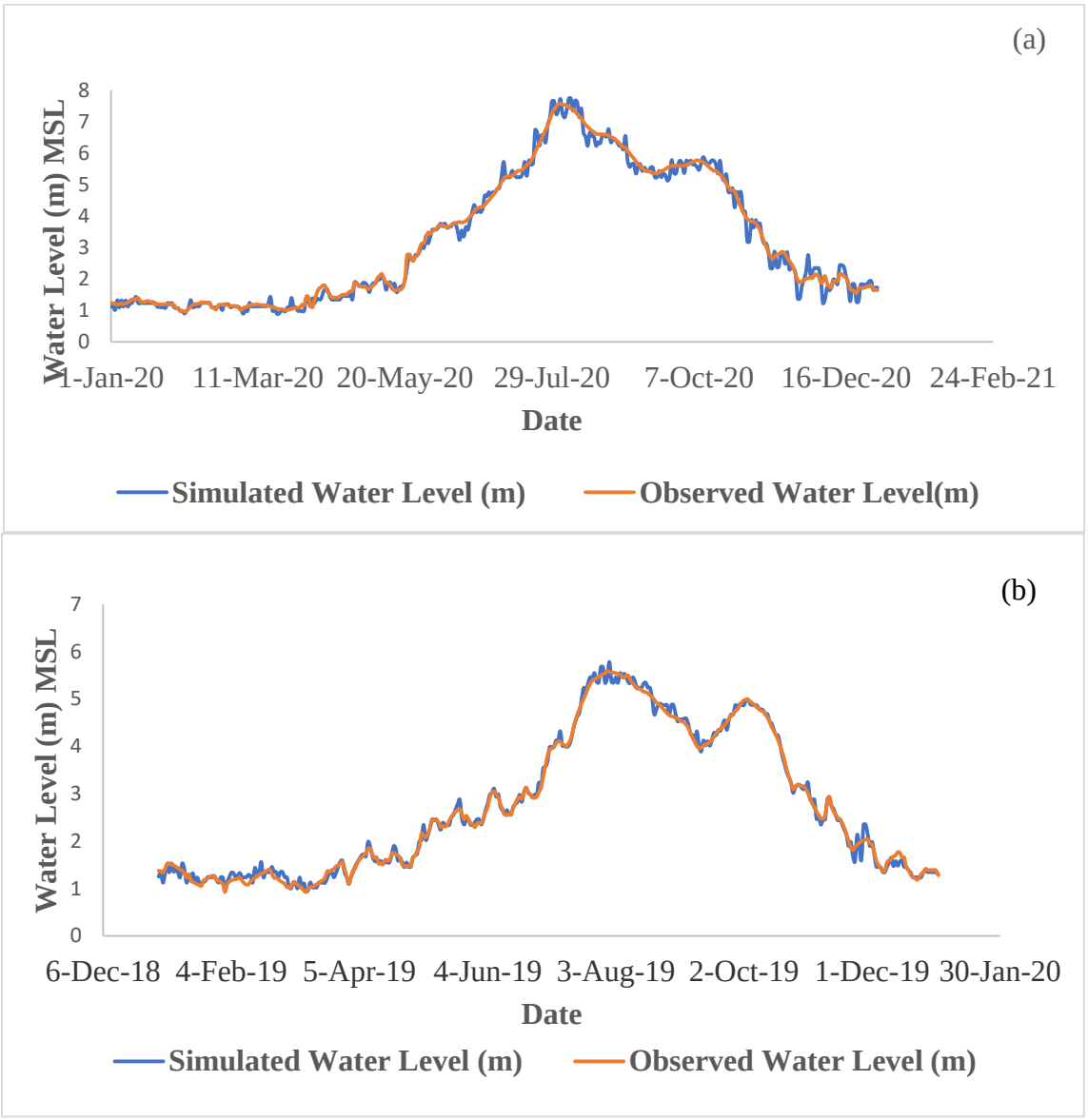

Figure 4: Comparison of observed and simulated water level hydrograph (a) the model was calibrated for the year of 2020 and (b) validated for the year of 2019

The model performance was evaluated using root mean squared error (RMSE) values. The RMSE values for the calibration and validation of hydrograph were 0.206 and 0.239, respectively, which indicate the simulated value is very close to observed value. In the 2D section of the model the Manning's roughness coefficient was assigned based on literature (Chow 1959), previous relevant studies (Horritt & Bates, 2002; Neal et al., 2010; Seyoum et al., 2011), and author's expert judgement. After the model calibration and validation, the unsteady flow simulation was performed using the values of the boundary hydrograph for the return periods of 100-year and 500-year. The estimated discharge values for the 100-year and 500-year return periods were used as the peak discharge for generating hydrograph with the interpolation technique in HEC-RAS. The simulation was performed for the monsoon period spanning from July to October. After performing the simulation, the data of the flood parameters (e.g., flood depth, velocity, and duration, etc.) were exported in tiff format in the ArcGIS environment for further post-processing. Finally, all the maps of the flood parameters were prepared in the ArcGIS environment.

Results and Discussion

Frequency Analysis

The flood frequency analysis and goodness-of-fit summary statistics (Table 1) based on the Chi-Square test show that the Pearson III frequency distribution function best fits the flood flow data (Figure 5). The minimum Chi-Squared test value for the Pearson III distribution indicates that it performs the best out of the five probability distribution functions. Gamma and Gumbel distributions are ranked second and third, respectively. The Log-Normal distribution performs the least of the five distributions (Table 1).

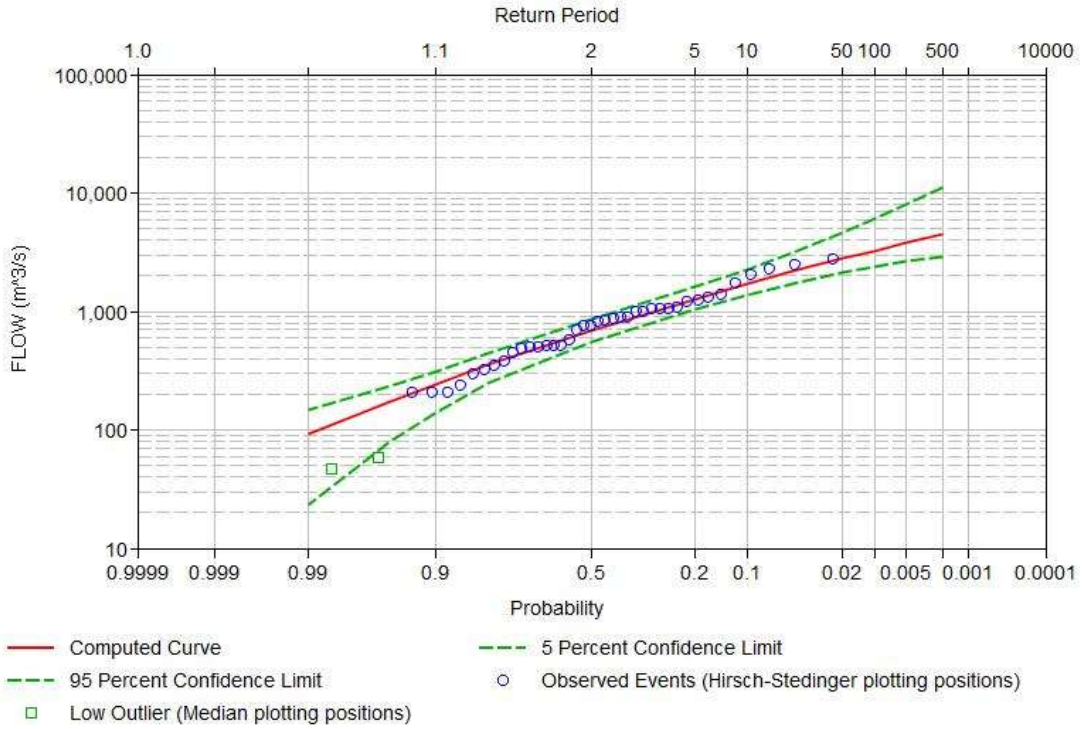

Figure 5: Pearson III distribution of river flow at Nayarhat station, Savar. This distribution function is the best fitted with the observed discharge data of Bangshi river at the selected station

Table 1: Goodness-of-fit test of river flow data for selecting most appropriate distribution function

PDF	Return Period		Chi-Square Test Statistics	Order
	100-year	500-year		
Pearson III	2882.8	3657.4	3.683	1
Gamma	2948.6	3782.9	5.634	2
Gumbel	2835.9	3629.9	5.634	3
Log Pearson III	3343.5	4754.5	4.073	4
Log Normal	4963.6	8092.6	4.854	5

The flood flow corresponding to the specific return periods is estimated using a 95% confidence interval. The flood flow values with a 95% confidence limit for 100-year and 500-year return periods using the Pearson III distribution are from 3373 to 2534 m^3/s and from 4313 to 3197 m^3/s, respectively (Table 2). The design

discharge values were used in the flood hydraulics model for assigning the boundary conditions of the model. The frequency distribution function using Log Pearson III distribution and Log-Normal distribution is shown in Appendix (A2 and A3), respectively. From Table 2, it is observed that the computed flow at the 500-year return period was 3657.4 m^3/s and the flow with the upper confidence limit was 4313.5 m^3/s for Pearson III distribution. From Figure 5, it is evident that the flood flow magnitude within the fifty years can be estimated more accurately using this range of data. With increasing the return period, the uncertainty of estimated values will also increase correspondingly. Therefore, the uncertainty should also be considered for estimating the approximate peak flood flow. It is also shown from Table 2 that the flood discharge values for the upper confidence level (e.g., 0.05) are larger than that of the lower confidence level (e.g., 0.95). The analysed flood flows for 100-year and 500-year return periods were subsequently used as the upstream boundary of the hydraulic model to determine the floodplain inundation.

Table 2: Summery of the flood flow frequency analysis using Pearson III distribution function

Computed Curve Flow (m^3/s)	Percent Change Exceedance	Confidence Limits		Return Period
		0.05	0.95	
3657.4	0.2	4313.5	3197.4	500
3219.8	0.5	3781.6	2823.4	200
2882.8	1	3373.2	2534.2	100
2539.2	2	2958.4	2237.8	50
2071	5	2397.5	1829.5	20
1701.4	10	1961.4	1500.6	10
1310.2	20	1512.3	1139.9	5
723.5	50	885.7	552	2

The computed flood flow shown in Table 2 represents the theoretically computed flow using the Pearson III distribution curve. The computed curve flow for 100-year and 500-year return periods are 3657.4 m^3/s and 2882.8 m^3/s, respectively. Figure 5 shows the observed point data is missing after 50-year return period and it may produce anomalies in estimating the theoretical distribution curve by extrapolation. In consequence, the computed flow for a longer return period (e.g., 500-year) may produce significant uncertainty in the computed results.

For flood flow frequency analysis of the hydrological data, it is required to have a complete intervention free-flow data of the catchment but the hydraulic structures (e.g., bridges) on the river may slightly change the flood flow behaviors (Odry and Arnaud 2017; Villarini et al. 2009). To address the issue, the hydrological model for computing the river flow data can be used in the hydraulic model in further study to show the extent of the inundation area. As climate change may increase the river flow during an extreme precipitation event, the river flow discharge was increased by up to 10% in performing the flood simulation.

Historical Flood Mapping

In the study area, the most devastating floods occurred in 1988 and 1998. The historical flood extent was therefore assessed for 1988 and 1998 based on the Landsat images for a specific union (e.g., Dhamsana) of the Savar upazila because a lot of industries are being developed in this area at the moment. As the cloud-free images are not available during the peak flood (e.g., at the time of maximum water level), the images were collected one week later from the maximum flood level to understand the extent of flood inundation. The flood extent shown in Figure 6 reveals that about 69% and 58% of the study area were flooded during the flood events of 1988 and 1998, respectively. The inundation area for the flood of 1988 is greater than the inundation area for the flood of 1998. But it is clearly shown in both maps (Figure 6) that most of the area was inundated during these flood events. Therefore, it should be mentioned here that the estimated flood extent shown in Figure 6 is underestimated. The inundation extent for 1998 may be greater than the inundated extent of 1988 because of the greater difference between the peak water level and image acquisition dates. The actual spatial extent of the flood will be greater than when the maximum flood water level occurs. The spatial extent of the flood could be estimated better if the radar satellite data (active sensor) was used, but there is no available free radar data at that time. The perennial water body was not differentiated in the delineation of the spatial extent of the flood. Figure 7 shows the historical flood water level hydrograph collected from the FFWC at different monitoring stations surrounding the study area. Appendix (A4) also shows that the flood level surrounding the monitoring station (Old Dhaleswari River at Jagir) exceeds the danger level at different years. The flood danger level at Nayarhat station, Savar, is 7.30 m above the PWD reference level. The highest flood water level recorded in this area was 9.9 m above the PWD reference level in 1988. Thus, the historical analysis shows that the most devastating floods occurred in the study area in the years 1988 and 1998.

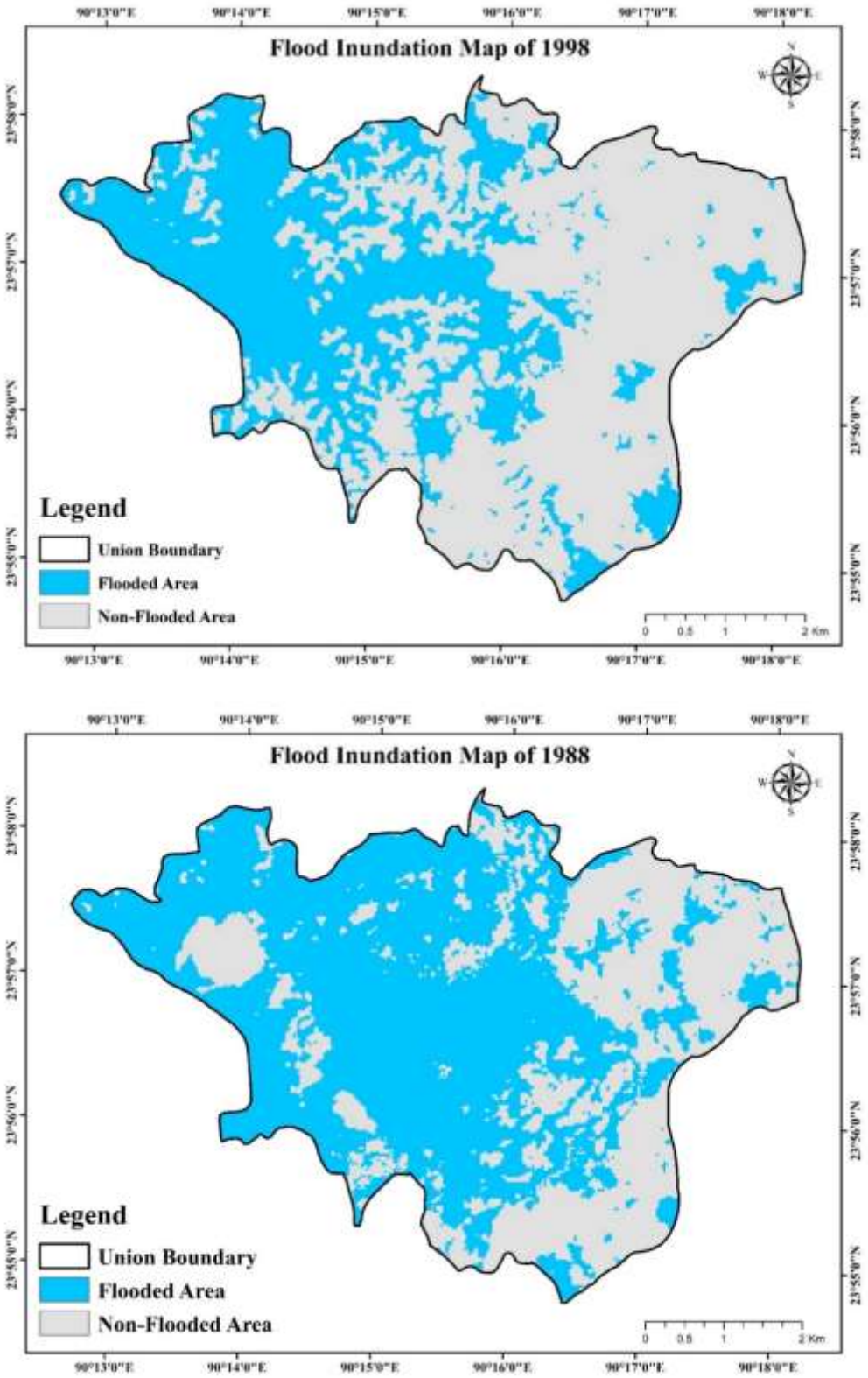

Figure 6: Flood inundation map of the study area for the flood events of 1998 and 1988 derived from Landsat 5 TM Satellite images. The flooded and non-flooded area was delineated using Normalized Difference Water Index (NDWI)

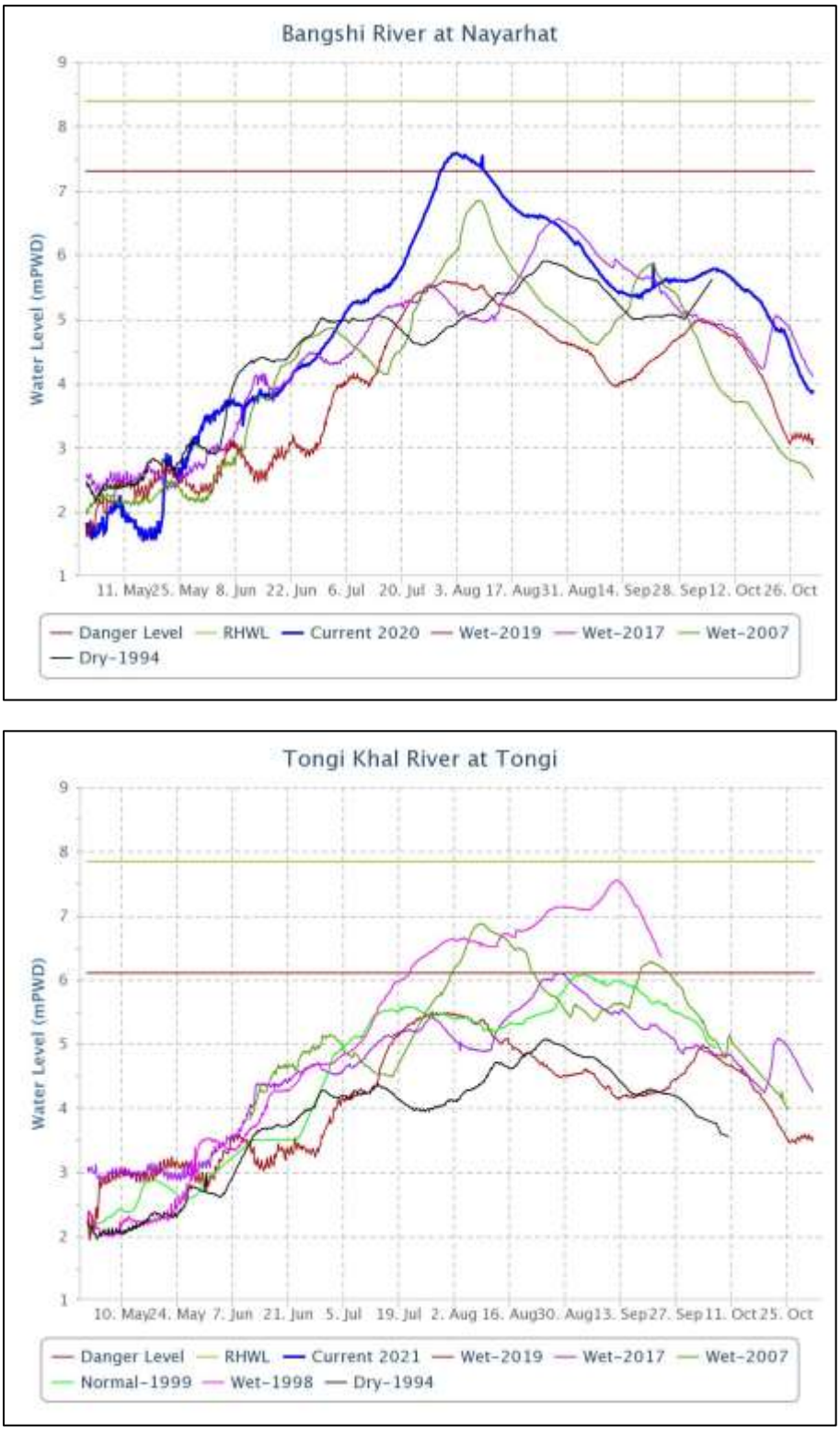

Figure 7: Water level hydrographs of the Bangshi River at Nayarhat and Tongi khal at Tongi (Source: FFWC)

The extent of the flood inundation in the study area is also consistent with some previous regional modelling studies (Faisal et al., 2003; Islam and Sado 2009; Mark et al. 2001). Although most parts of the study areas are vulnerable to flood, many industrial development activities are continuously being implemented within the study area without considering the flood assessment. With increasing urban development, the magnitude of the flood may be intensified. Therefore, for urban and industrial development within the study area, flood hazard and risk assessment results should be taken into consideration.

Flood Hazard Mapping
Water Depth-based Estimation

The historical flood level at the nearby station (SW 14.5, Nayarhat) indicates that the flood level exceeds the danger level in different historical flood events. The flood extent of two extreme flood events that occurred in Bangladesh in 1988 and 1998 shown in Figure 6 indicates that most of the area of the study area was flooded. The historical maximum flood elevation during the 1988 year was 9.9 m PWD at the nearby monitoring station. The maximum topographic elevation of the study area is 10.29 m, and most of the area was below the maximum water level elevation recorded. Therefore, the historical flood extent map shown in Figure 6 is very reasonable because most of the study area was flooded during the flood events of 1988 and 1998. It is also clear that the flood extent in 1988 was greater than that in 1998 because the maximum flood elevation that occurred in 1988 was higher than that in 1998. Although the study area is situated within the catchment of both the Bangshi and Turag rivers, the study area is very close to the Bangshi River and is directly connected to it by different drainage channels. Therefore, there is a little probability of the occurrence of a flood in the study area due to the influence of the Turag River. The topographic elevation is also higher in the western part of the Turag River, which acts as a barrier for the flood to occur in the study area due to the influence of the Turag River.

The flood depth within the model domain was calculated by the hydraulic model. Flood depth data is extracted from the HEC-RAS hydraulic model into the ArcGIS interface in tiff format. The flood depth is estimated by the difference between the simulated water surface elevation and the ground elevation. The water surface elevation is calculated using the unsteady flow equation for each numerical mesh. The extracted flood depth data is post-processed using ArcGIS and, finally, the flood depth map is prepared. The flood depth maps for the 100-year return period are shown in Figure 8. As the regional topography data used in the model was of very coarse resolution (30 m), the produced flood inundation depth may have some anomalies in the floodplain area.

The maximum flood depth shown in Figure 8 is 7.89, which is located at the river channel or any topographic depression within the whole model domain area. From Figure 8 and Figure 9, it is evident that the design flood level for 100-year and 500-year return periods has overtopped some parts of Baipail Road. The overtopped location of the road is located at the culvert site of the highway, where the drainage channel crosses the road network through the culvert. The topographic elevation of the road at the culvert side is comparatively lower than the remaining part of the road. Figure 9 shows the flood inundation depth for a 500-year return period, and it is clear from the figure that the flood extent of the study area is increased significantly for a 500-year return flood. The simulated result shows that about 68% and 79% of the study area will be inundated by the floods of 100-year and 500-year return periods, respectively. The highest flood depth that occurs within the river channel is about 8.67 m. It is clear from Figure 9 that the road network will be overtopped at different locations during the 500-year flood level. The flood-free zone in the study area will be significantly decreased during the 500-year flood event. Therefore, for both the 100-year and 500-year return periods, flooding could seriously affect the study area.

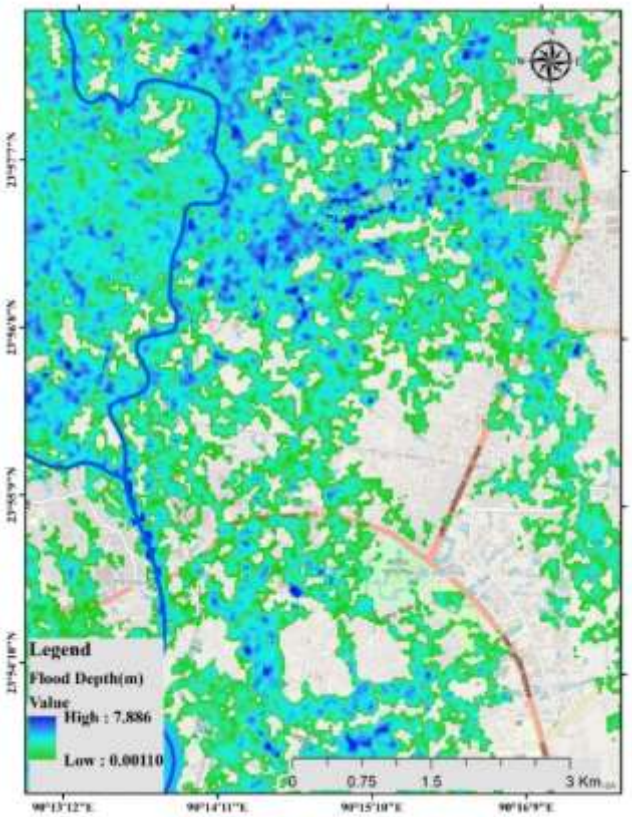

Figure 8: The maximum flood inundation depth map for 100-year return period

Velocity-based Estimation

Flood velocity is an important hydraulic characteristic for understanding flood damage. However, flow velocity may cause additional damage to the foundation and infrastructure, particularly in steep slope areas. With the lower discharges corresponding to lower water velocities and shallower water depths, the flooding becomes relatively safer. At a low depth, it may not be life-endangering, but it could still result in considerable damage to property. The simulated flood flow velocity of the drainage channel passing through the floodplain area far away from the main river channel during the flood event of 2020 was shown in Figure 10 and Figure 11 at the upstream and downstream sections of a canal flowing beside Baipail Road. The maximum velocity at the upstream and downstream sections of the canal is 0.065

m/s and 0.045 m/s, respectively. The flood velocity maps were prepared for 100-year and 500-year flood events, shown in Figure 12 and Figure 13, respectively. The flood velocity in the study area is very low because the topography of the study area is almost flat. Therefore, the flood flow velocity in the floodplain is somewhat lower than the flood flow velocity in the main river channel. The slope of the river channel is very gentle, and it increases towards the downstream section of the Bangshi River.

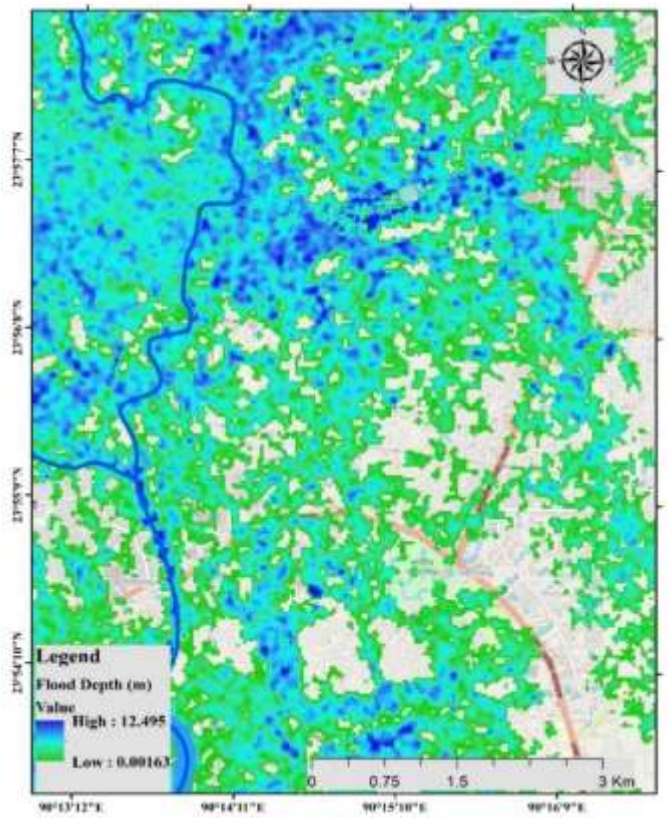

Figure 9: The maximum flood inundation depth map for 500-year return period

Figure 12 shows the flood flow velocity for the 100-year return period. It is clearly shown from Figure 12 that the flow velocity in the upstream channel is comparatively lower than the downstream section because the slope of the channel in the downstream is steeper. The maximum flood flow velocity for the 100-year return period is 2.31 m/s. The minimum flood flow velocity was close to zero. From Figure 13, it is also shown that the flood flow velocity increases slightly within the study area for a 500- year flood event. The maximum flood flow velocity is 4.52 m/s for a 500-year flood. Flood flow velocity in the other parts of the study area varies differently. The spatial variability of the flow velocity is shown at a different section of the model domain (Figure 13). Figure 13 also shows that flood flow velocity is increased significantly at different locations in the study area during the flood event of the 500-year return period. The increase in flood flow velocity for the 500-year return period is due to an increase in the upstream discharge assigned as the boundary condition.

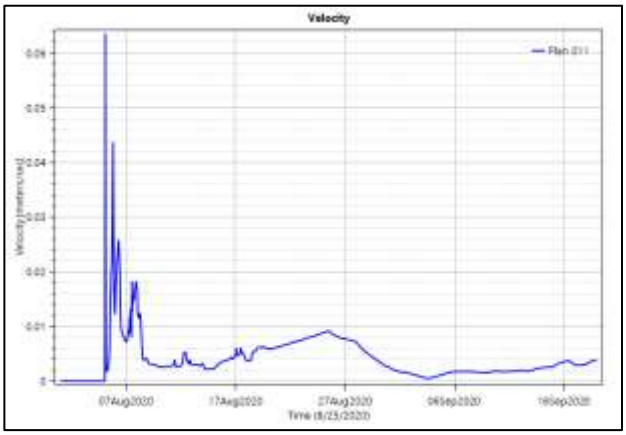

Figure 10: Simulated flood velocity at the upstream section of the canal flowing beside Baipail Road during 2020 flood event.

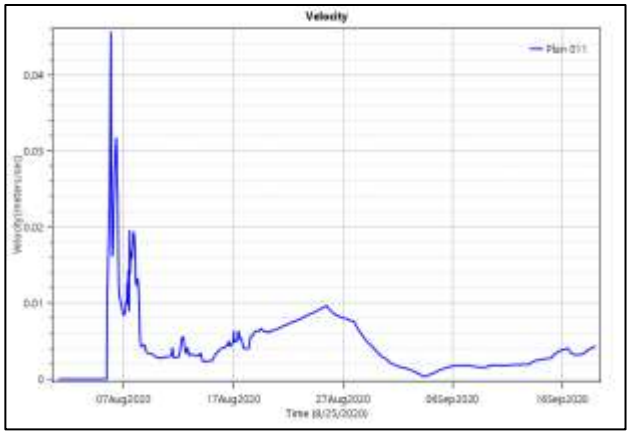

Figure 11: Simulated flood velocity at the downstream section of the canal flowing beside Baipail Road during 2020 flood event

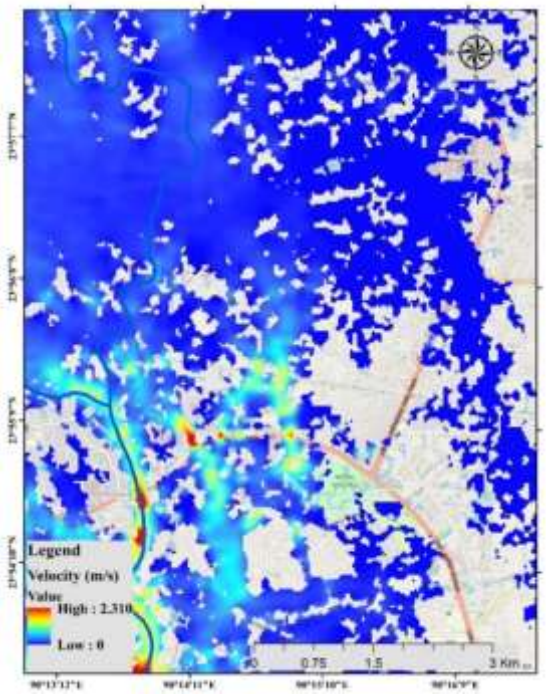

Figure 12: The maximum flood velocity for 100-year return period at study area

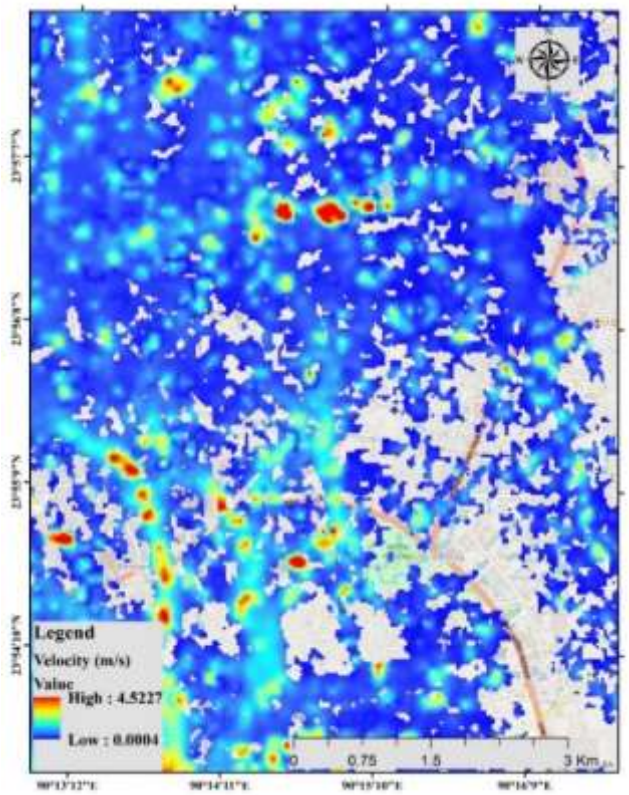

Figure 13: The maximum flood velocity for 500-year return period in the study area

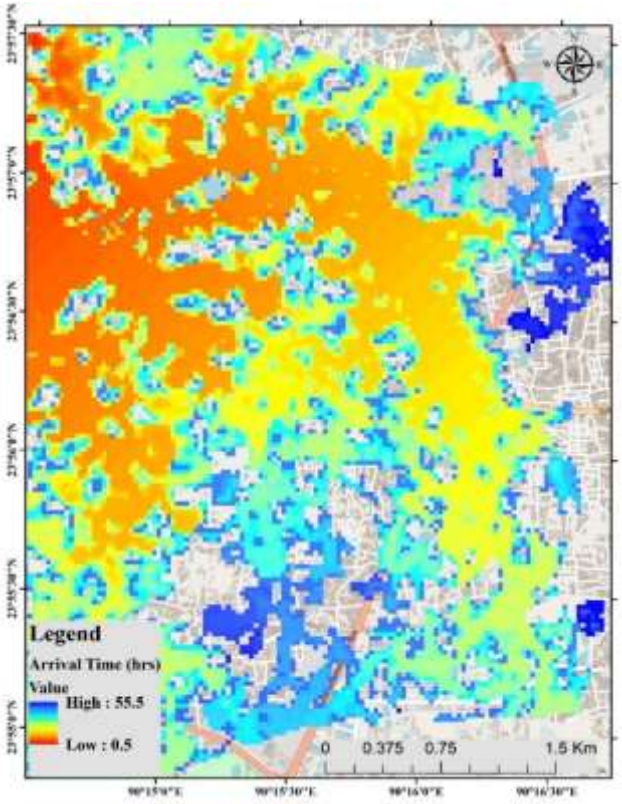

Figure 14: The flood arrival time for 1 m flood depth from the start time of the simulation. The flood arrival time indicates the rate of the onset of the flooding

The flood arrival time is one of the important hydraulic characteristics for making preparedness and reducing the risk of flooding. The flood arrival time was exported from the HEC-RAS model as a raster format into ArcGIS and finally prepared the flood arrival time map. For exporting the flood arrival time from the start time of the simulation, the threshold depth (1 m) was assigned as the parameter. Figure 14 shows the flood arrival time for a 1 m flood depth from the start of the simulation. The onset of the flooding depends on multiple factors of hydrology and hydraulics in the study area. Figure 14 shows that the arrival time is increasing with increasing distance from the river. The flood arrival time at the highly elevated area is greater than the low-lying area. The little arrival time indicates that the area is more vulnerable to flooding than the higher flood arrival time.

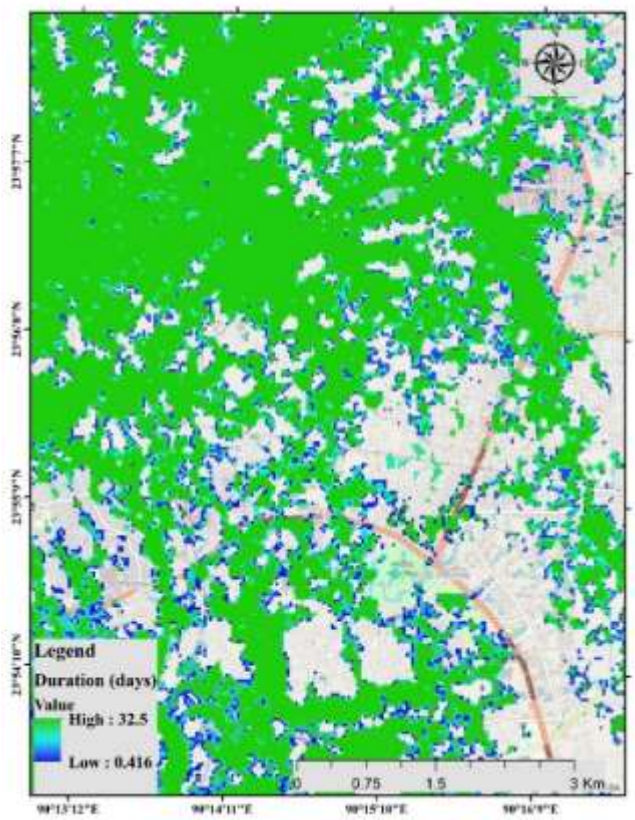

Figure 15: The duration of the flood map for 1m depth at 100-year return period. This map indicates the length of the time a location is inundated to 1m depth flood

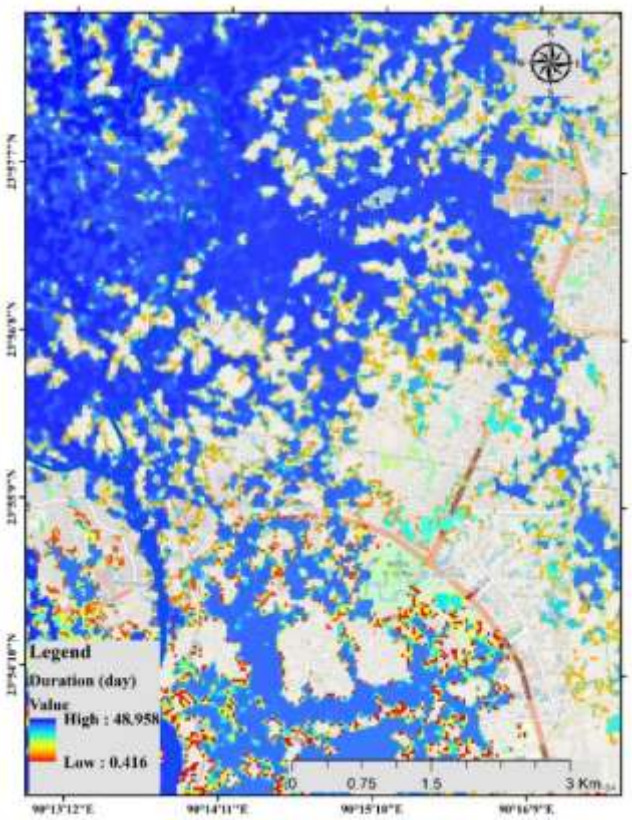

Figure 16: The duration of the flood map for 1m depth at 500-year return period. This map indicates the length of the time a location is inundated to 1m depth flood

Flood Duration-based Estimation

The flood duration is also an important output parameter of the hydraulic model. The duration of the flood mostly depends on the hydraulics of the river channel and floodplain area. The flood duration of 100-year and 500-year return periods was estimated from the hydraulic model. Figure 15 shows the flood flow duration map for the 100-year return period, and the maximum flood duration for 1 m depth is 32.5 days. It indicates that the length of time a location is inundated to a 1 m depth flood level. The minimum duration is 1 day for 1 m of depth at a location that is inundated. It is shown from the map that the duration of the flood in the highly elevated area is very low and the duration of the flood in the low-lying topographic area is higher. The flood duration for a 500-year flood is shown in Figure 16, and the maximum duration for a 1 m depth flood is 48.958 days and the minimum duration is 0.416 days. The higher flood duration is very harmful to the built infrastructure. The higher flood duration may cause significant damage to the built environment and any commercial and industrial activities. The flood flow duration also depends on multiple factors, which should be taken into consideration.

Conclusions

The present study was conducted for flood hazard assessment in the Bangshi River drainage basin. The historical flood extent analysed from the remote sensing data of Landsat satellite images shows that most parts of the study area are flooded during the major flood events in Bangladesh. The flood flow data was fitted with different analytical frequency distribution functions, and it shows that the Pearson III distribution function best fits with the observed data based on the Chi-Squared statistical test. The model was simulated with an estimated flow of 100-year and 500-year return periods. The analysis of the historical flood data shows that the water level exceeds the danger level at the nearby monitoring station of the study area in different years. The devastating flood occurred in the study area in the years 1988 and 1998. The maximum flood level was 9.9 m during the flood event of 1988. The Landsat satellite image analysis also shows that most parts of the study area was flooded during the floods of 1988 and 1998. For a 100-year return period, about 68% of the area will be inundated, and for a 500-year return period, 79% of the area will be inundated. The maximum flood velocity for the 100 year and 500-year return periods is 2.31 m/s and 4.52 m/s, respectively. The flood duration for the 100-year and 500-year return periods is about 32.5 and 48.95 days, respectively. The

simulated flood depth can be used for any urban and industrial development within the study area. If the land elevation is raised above the simulated flood elevation, the buildings and other infrastructure will be safe from the flood hazard.

Acknowledgements

The authors would like to acknowledge the Department of Disaster Science and Climate Resilience, University of Dhaka, for giving all supports to conduct this research in the department. They are also grateful to the Bangladesh Water Development Board (BWDB) for providing the river discharge, water level, and cross-section data for this study.

References

Abedin, M. A., Colllins, A. E., Habiba, U., and Shaw, R. (2019). Climate Change, Water Scarcity, and Health Adaptation in Southwestern Coastal Bangladesh, International Journal of Disaster Risk Science 10(1), pp.28-42. doi: 10.1007/s13753-018-0211-8.

Baidya, S., Singh, A. and Panda, S. N. (2020). Flood Frequency Analysis, Natural Hazards, 100(3), pp.1137-1158. doi: 10.1007/s11069-019-03853-4.

Chow, V. T. (1951). A General Formula for Hydrologic Frequency Analysis, Eos, Transactions American Geophysical Union 32(2), pp. 231–237. doi: 10.1029/TR032I002P00231.

Chow, V. T. (1959). Open-Channel Hydraulics. McGraw-Hill Civil Engineering Series 680.

Delaporte, I., and Maurel. M. (2018). Adaptation to Climate Change in Bangladesh, Climate Policy 18(1), pp.49-62. doi: 10.1080/14693062.2016.1222261.

Dewan, A. M., Nishigaki, M. and Komatsu, M. (2004). DEM Based Flood Extent Delineation in Dhaka City, Bangladesh, Journal of the Faculty of Environmental Science and Technology 9(1), pp. 99-110.

Faisal, I.M., Kabir, M.R. and Nishat, A., (2003). The disastrous flood of 1998 and long-term mitigation strategies for Dhaka City, In Flood Problem and Management in South Asia, pp. 85-99.

Foody, G. M. (2002). Status of Land Cover Classification Accuracy Assessment. Remote Sensing of Environment, 80(1), pp.185-201.

Gao, B. C. (1996). NDWI—A Normalized Difference Water Index for Remote Sensing of Vegetation Liquid Water from Space, Remote Sensing of Environment, Vol. 2480, pp. 225-236.

Grimaldi, S., Kao, S. C., Castellarin, A., Papalexiou, S. M., Viglione, A., Laio, F., Aksoy, H. and Gedikli, A. (2011). Statistical Hydrology, in Treatise on Water Science. Vol. 2.

Lane, B, (2002). Statistical methods in hydrology. doi: 10.1201/9780429423116-36.

Harris, J., Brunner, G. and Faber, B. (2008). Statistical software package, World Environmental and Water Resources Congress 2008: Ahupua'A, pp. 1-10. doi: 10.1061/40976(316)568.

Hoque, M. A. A., Pradhan, B., Ahmed, N. and Roy, S. (2019). Tropical cyclone risk assessment using geospatial techniques for the eastern coastal region of Bangladesh, Science of the Total Environment, 692, pp.10-22. doi: 10.1016/j.scitotenv.2019.07.132.

Horritt, M. S. and Bates, P. D., (2002). Evaluation of 1D and 2D numerical models for predicting river flood inundation, Journal of Hydrology, 268(1-4), pp.87-99.

Hossain, J., Salehin, M. and Mourin, M. M. (2017). Impact of storm surge flooding on groundwater salinity in the polder protected and non-polder area of coastal aquifer in Bangladesh, In Proceedings of the International Conference on Disaster Risk Mitigation, BUET, Dhaka, Bangladesh, pp. 23-24.

Huq, M., Cheng, Q., Altan, O., Shoeb, A. Z. M., Hossain, M. A., Sarker, M., Islam, N., Saleem, N., Javed, A., Longg, X. and Dughairi, A. A. A. (2020). Assessing vulnerability for inhabitants of Dhaka City considering flood-hazard exposure, Geofizika, 37(2), pp.97-130. doi: 10.15233/gfz.2020.37.5.

Islam, M. and Sado, K. (2000). Flood hazard assessment for the construction of flood hazard map and land development priority map using NOAA/AVHRR data and GIS–a case study in Bangladesh, Hydrological Sciences–Journal–des Sciences Hydrologiques, 45(3), pp.337-357.

Jain, S. K., Singh, R. D., Jain, M. K. and Lohani, A. K. (2005). Delineation of flood-prone areas using remote sensing techniques, Water Resources Management, 19(4), pp.333-347.

Kamrujjaman, M. and Nabi, M. R. (2015). Ichthyodiversity of the Bangshi river, Savar, Dhaka, Jahangirnagar University Journal of Biological Sciences, 4(1), pp.19-25.

Karim, M. A. and Chowdhury, J. U. (1995). A comparison of four distributions used in flood frequency analysis in Bangladesh, Hydrological Sciences Journal, 40(1), pp.55-66.

Liserio Jr, F. F. and Mahan, P. W. (2019). Manage the Risks of Severe Wind and Flood Events, Chemical Engineering Progress, 115(4), pp.42-49.

Mark, O., Apirumanekul, C., Kamal, M. M. and Praydal, G. (2001). Modelling of urban flooding in Dhaka City. Urban Drainage Modeling, pp. 333-343.

Masood, M. and Takeuchi, K. (2012). Assessment of flood hazard, vulnerability and risk of mid-eastern Dhaka using DEM and 1D hydrodynamic model, Natural Hazards, 61(2), pp.757-770.

McFeeters, S. K. (1996). The use of the Normalized Difference Water Index (NDWI) in the delineation of open water features, International Journal of Remote sensing, 17(7), pp.1425-1432.

Mondal, M. S. H., Murayama, T. and Nishikizawa, S. (2021). Examining the determinants of flood risk mitigation measures at the household level in Bangladesh. International Journal of Disaster Risk Reduction, 64, p.102492.

Hossain, M. D., Rahman, M. M., Chandra, J. B., Shammi, M. and Uddin, M. K. (2012). Present status of water quality of the Bangshi River, Savar, Dhaka, Bangladesh, Bangladesh Journal of Environmental Research, 10, pp.17-30.

Mourin, M. M., Ferdaus, A. A. and Hossain, M. J. (2017). Landslide Susceptibility Assessment in Chittagong District of Bangladesh Using Adaptive Neuro Fuzzy Inference System (ANFIS) and GIS, In Proceedings of the International Conference on Disaster Risk Mitigation, Dhaka, Bangladesh, pp. 23-24.

Mourin, M. M., Ferdaus, A. A. and Hossain, M. J. (2018). Landslide Susceptibility Mapping in Chittagong District of Bangladesh using Support Vector Machine integrated with GIS, In International Conference on Innovation in Engineering and Technology (ICIET), pp. 1-5. IEEE. doi: 10.1109/CIET.2018.8660782.

Munasinghe, D., Cohen, S., Huang, Y.F., Tsang, Y.P., Zhang, J. and Fang, Z (2018). Intercomparison of satellite remote sensing-based flood inundation mapping techniques, JAWRA Journal of the American Water Resources Association, 54(4), pp.834-846.

Naghettini, M. (2017). Fundamentals of Statistical Hydrology, Cham: Springer International Publishing.

Neal, J. C., Fewtrell, T. J., Bates, P. D. and Wright, N. G. (2010). A comparison of three parallelisation methods for 2D flood inundation models, Environmental Modelling & Software, 25(4), pp.398-411.

Odry, J. and Arnaud, P. (2017). Comparison of flood frequency analysis methods for ungauged catchments in France, Geosciences, 7(3), p.88.

Okubo, K., Khan, M. and Hassan, M. Q. (2010). Hydrological processes of adsorption, sedimentation, and infiltration into the lake bed during the 2004 urban flood in Dhaka city, Bangladesh, Environmental Earth Sciences, 60(1), pp.95-106.

Rahman, M. S., Molla, A. H., Saha, N. and Rahman, A. (2012). Study on heavy metals levels and its risk assessment in some edible fishes from Bangshi River, Savar, Dhaka, Bangladesh, Food Chemistry, 134(4), pp.1847-1854.

Rahman, M. M., Arya, D. S., Goel, N. K. and Dhamy, A. P. (2011). Design flow and stage computations in the Teesta River, Bangladesh using Frequency Analysis and MIKE 11 Modeling, Journal of Hydrologic Engineering, 16(2), pp.176-186.

Rasid, H. and Paul, B. K. (1987). Flood problems in Bangladesh: is there an indigenous solution? Environmental Management, 11(2), pp.155-173.

Rimi, R. H., Haustein, K., Allen, M. R. and Barbour, E. J. (2019). Risks of pre-monsoon extreme rainfall events of Bangladesh: Is anthropogenic climate change playing a role, Bull. Am. Meteorol. Soc, 100(1), pp. S61-S65.

Roy, B., Khan, M., Mostafa, S., Islam, A. K. M., Mohammed, K., Khan, M. and Uddin, J. (2021). Climate-induced flood inundation for the Arial Khan River of Bangladesh using open-source SWAT and HEC-RAS model for RCP8. 5-SSP5 scenario, SN Applied Sciences, 3(6), pp.1-13.

Roy, B., Islam, A. S., Islam, G. T., Khan, M. J. U., Bhattacharya, B., Ali, M. H., Khan, A. S., Hossain, M. S., Sarker, G. C. and Pieu, N. M. (2019). Frequency analysis of flash floods for establishing new danger levels for the rivers in the northeast haor region of Bangladesh, Journal of Hydrologic Engineering, 24(4), p.05019004.

Sampson, C. C., Smith, A. M., Bates, P. D., Neal, J. C., Alfieri, L. and Freer, J. E. (2015). A high-resolution global flood hazard model, Water Resources Research, 51(9), pp.7358-7381.

Seyoum, S. D., Vojinovic, Z., Price, R. K. and Weesakul, S. (2012). Coupled 1D and noninertia 2D flood inundation model for simulation of urban flooding, Journal of Hydraulic Engineering, 138(1), pp.23-34.

Shaw, R. (2006). Critical issues of community-based flood mitigation: examples from Bangladesh and Vietnam, Science and Culture, 72(1/2), p.62.

Solomon, S., Qin, D., Manning, M., Chen, Z., Marquis, M., Averyt, K. B., Tignor, M. and Miller, H. L. (2007). Summary for policymakers, Climate Change, pp.1-18.

Srivatsav, N., Jaxa-Rozen, M. and Van Staveren, R. (2014). Using microfinance for flood mitigation and climate adaptation in Bangladesh, In 32nd International Conference of the System Dynamics Society, Delft, The Netherlands.

Uddin, K. and Matin, M.A. (2021). Potential flood hazard zonation and flood shelter suitability mapping for disaster risk mitigation in Bangladesh using geospatial technology. Progress in disaster science, 11, p.100185.

Ul Hassan, M., Hayat, O. and Noreen, Z (2019). Selecting the best probability distribution for at-site flood frequency analysis; a study of Torne River, SN Applied Sciences, 1(12), pp.1-10.

Villarini, G., Smith, J. A., Serinaldi, F., Bales, J., Bates, P. D. and Krajewski, W. F. (2009). Flood frequency analysis for nonstationary annual peak records in an urban drainage basin. Advances in water resources, 32(8), pp.1255-1266.

Wax, E. (2007). In flood-prone Bangladesh, a future that floats. The Washington Post.

Xu, H. (2006). Modification of normalised difference water index (NDWI) to enhance open water features in remotely sensed imagery, International Journal of Remote Sensing, 27(14), pp.3025-3033.

Younus, M. A. F. (2014). Flood vulnerability and adaptation to climate change in Bangladesh: a review. Journal of Environmental Assessment Policy and Management, 16(03), p.1450024.

Appendix

A1: Methodology of Landuse and Landcover Map Preparation

The land use and land cover map of Dhamrai and Savar upazilas where the focused study site is located was prepared from the Landsat-8 Operational Land Imager (OLI) scene (acquisition date 2020/01/10, Row 43 and path 137) with 30 m spatial resolution. The images pre-processing (geometric, radiometric, and atmospheric correction) was performed using ArcGIS 10.8 software. The land use and land cover of the study area was classified into five classes (water body, agricultural land, rural settlement, vegetation, bare soil, and built-up area) using hybrid classification scheme. Firstly, the potential land use class was identified using the unsupervised clustering algorithm. Then, the training sample was selected for supervised classification using maximum likelihood classification algorithm (Hoque et al. 2019). The accuracy of the image classification was determined using the random points from the google earth images of the same period. The stratified random sampling technique was used to generate the sampling point with minimum 50 points for each land use and land cover class. The total 350

random point was generated and used in in the accuracy assessment. We followed the accuracy assessment technique explained by Foody, 2002. The produced land use and land cover map show that the overall accuracy was 91.38% and Kappa coefficient value was 92.05%.

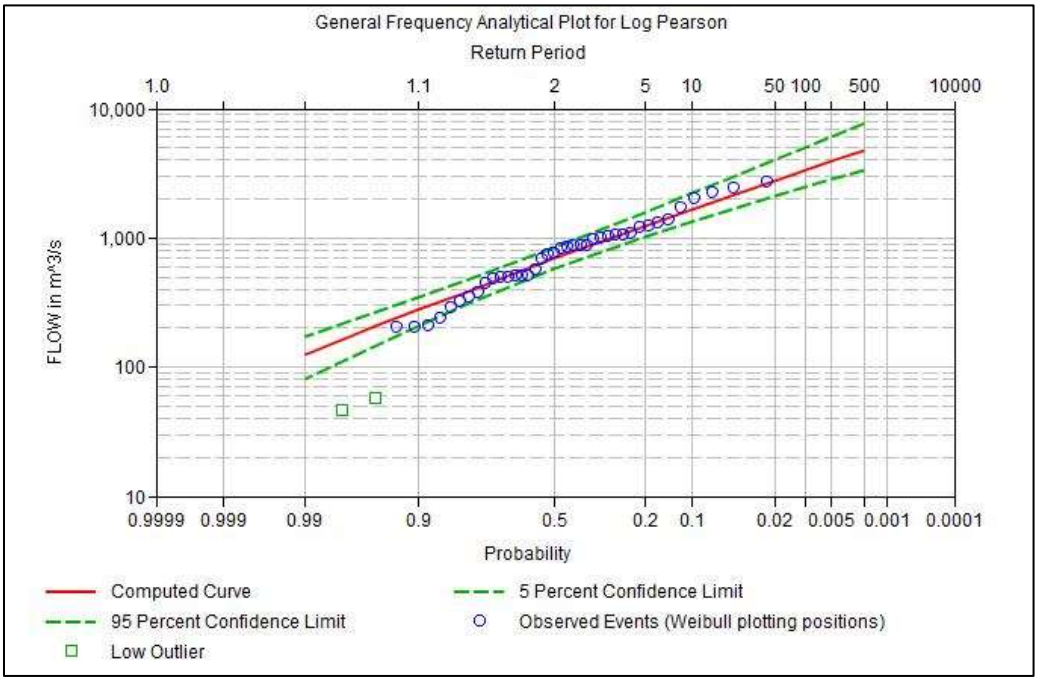

A2: Peak flood flow frequency distribution of the Bangshi River at Nayarhat station, Savar using Log Pearson III distribution

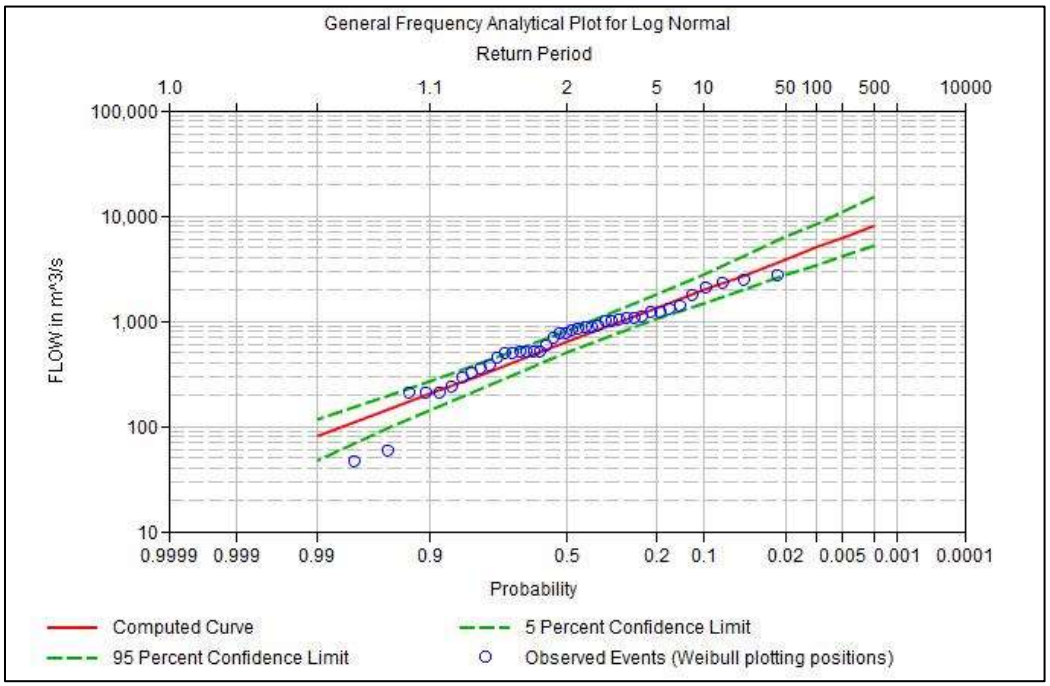

A3: Peak flood flow frequency distribution of the Bangshi River at Nayarhat station, Savar using Log Normal distribution

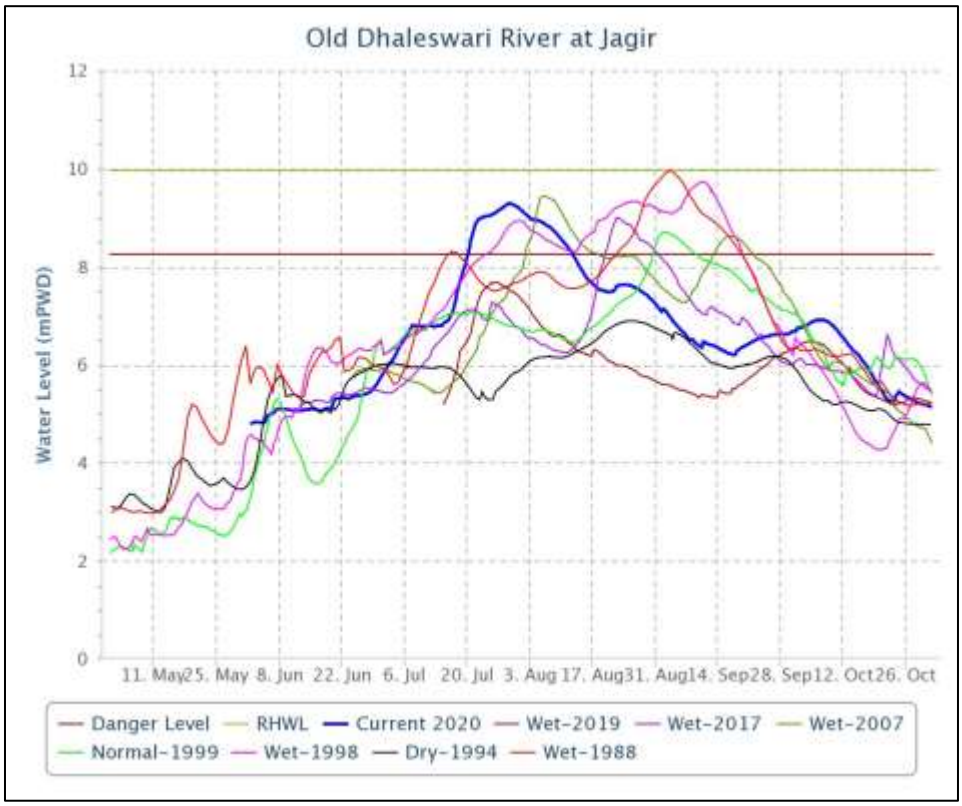

A4: Water level hydrographs of the Old Dhaleswari River at Jagir. The water level at the station exceeds the danger level during the major flood in Bangladesh (Source: FFWC)

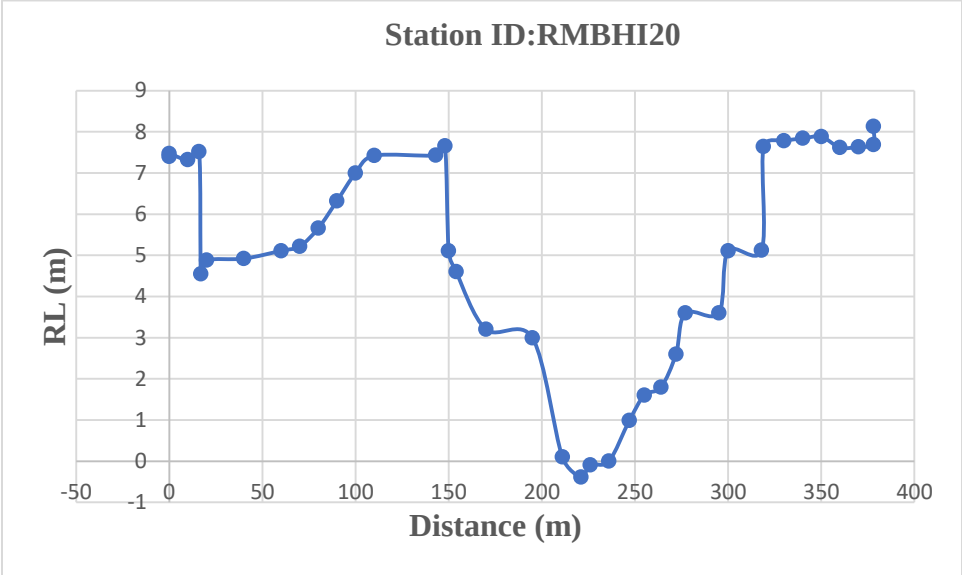

A5.1: Cross-section of the Bangshi River at Mirzapur, Tangail.

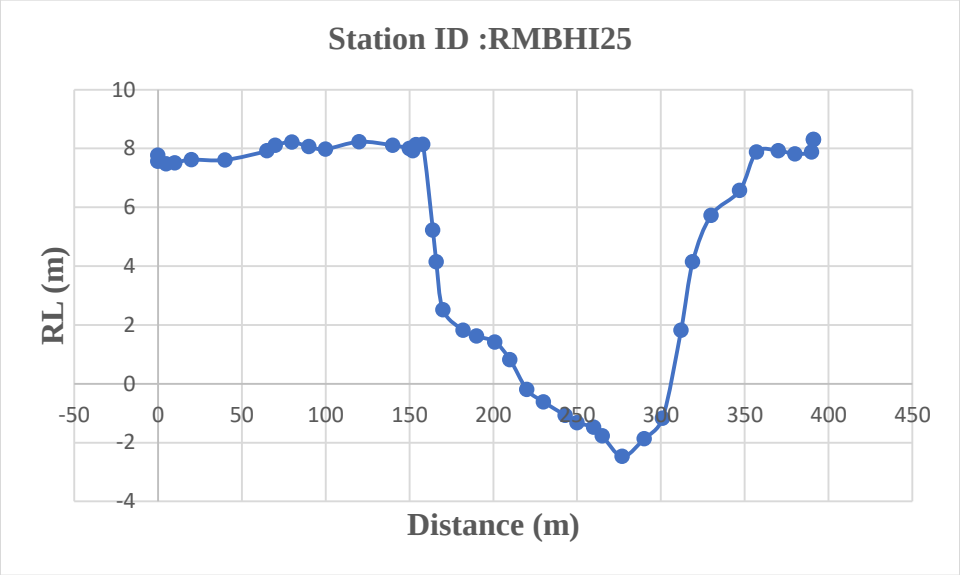

A5.2: Cross-section of the Bangshi River at Dhamrai, Dhaka

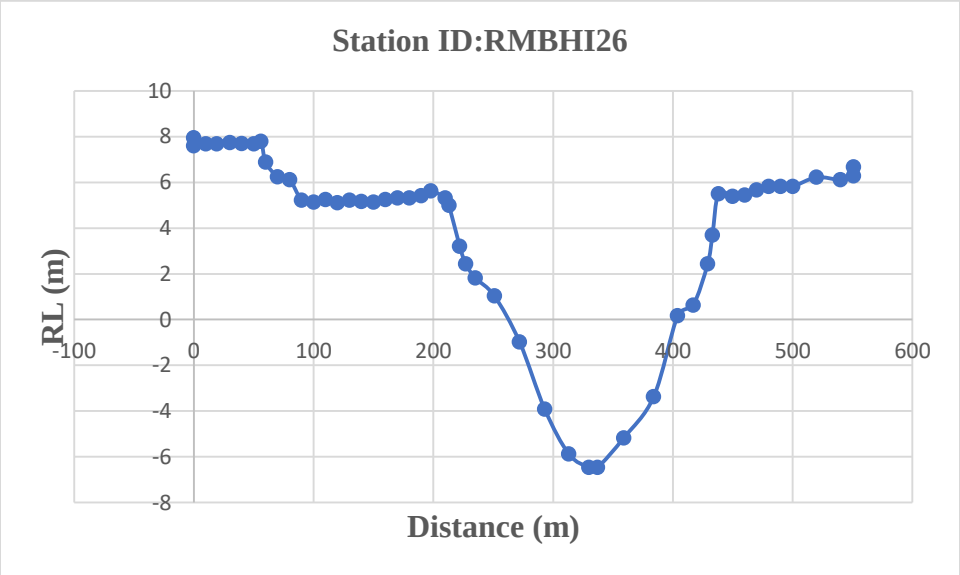

A5.3: Cross-section of the Bangshi River at Savar, Dhaka

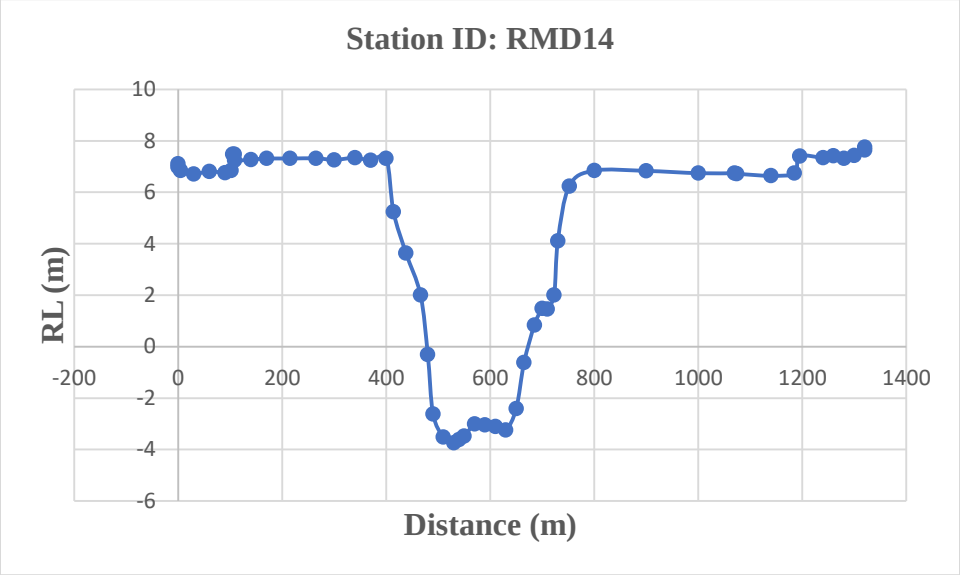

A5.4: Cross-section of the Bangshi River at Savar, Dhaka